Geomechanics and Engineering, *Vol. 25, No. 5 (2021) 395-403*
DOI: https://doi.org/10.12989/gae.2021.25.5.395

Application of artificial neural network for prediction of flow ability of soft soil subjected to vibrations

Guangjian Xiang[1], Deshun Yin*[1], Chenxi Cao[1] and Lili Yuan[2]

[1]*College of Mechanics and Materials, Hohai University, Nanjing 211100, China*
[2]*Shenzhen Guoyi Park Construction Co., LTD, Shenzhen 518000, China*

(Received June 21, 2020, Revised May 21, 2021, Accepted June 2, 2021)

Abstract. Vibrations induced by the operation of underground trains result in certain changes in the flow characteristics of the underground soft soil, which may lead to problems like ground settlement and damages of subway tunnels. In this study, an improved drag-sphere device is implemented to investigate the flow ability of soft soil subjected to vibrations, and the experimental results indicate that vibrations with high frequencies and low confining pressure enhanced the flow ability of soil samples. Then an artificial neural network (ANN) model is developed based on the obtained experimental data to predict the soil viscosity, where the genetic algorithm (GA) is implemented to optimize the weights and biases in the network. Specifically, by comparing the simulated results with experimental data, the optimal topology, training algorithm, and transfer functions are selected for the proposed model, and the model predictions are in high agreement with the experimental data, which denotes the proposed ANN model is accurate and reliable. Moreover, an analysis on the contributions of each input reveals that the water content affects the soil viscosity most while the frequency has the least impact for a single factor, which is in correspondence with the fact that the flow ability of soft soil is mainly affected by the geological conditions and its natural properties.

Keywords: flow ability; artificial neural network; soft soil; genetic algorithm

1. Introduction

Over the past years, as the urban population keeps growing, the rising traffic congestion and carbon emission have been major concerns in China's metropolitans. To reduce the traffic pressure, underground rail transit systems have been widely established in many cities located in the Yangtze River Delta (Yang and Hung 2008). However, as many underground railway stations and tunnels are built in soft soil, vibration induced by the operation of the subways result in problems like soil liquidation and damages of soil structure, ultimately leading to ground settlement and other engineering accidents (Kheirbek and Fleureau 2012, Xu *et al.* 2016). This is because soft soil distributed in many deltas and floodplains generally exhibits high compressibility, low shear strength, poor bearing capacity, high water content, and typical rheological behaviors (Al-Bared *et al.* 2019, Huang *et al.* 2020, Zhu *et al.* 2019). Thus, to achieve soil improvement and safe operation of subways, studies on measuring and evaluating the mechanical properties of soft soil subjected to vibrations are indispensable.

Previous researchers have been focused on the evaluation of mechanical properties and flow characteristics of soft soil subjected to vibrations, which are the underlying causes of subgrade settlement and structural failure (Huang *et al.* 2015, Shih *et al.* 2017). Traditionally, considering the difficulty of field observation, two sorts of laboratory tests, shaking table tests and dynamic triaxial tests, are commonly used to provide empirical data (Liu *et al.* 2010, Moss and Crosariol 2013). According to Chen *et al.* (2012), the dynamic response of ground soft soil can be obtained through a series of shaking table tests, and the results demonstrate that the frequency of input motions and the pore pressure of soil significantly affect the performance of both the soft foundation and the structure. Kumar *et al.* (2018) established a dynamic model of coercive soil based on the results of the dynamic triaxial tests, which is in agreement with the ground response analysis of the region. Unfortunately, these experimental methods have always treated the soil specimen as a whole and the loads were applied from outside, ignoring the fact that the vibrations induced by the operation of underground trains come from inside the foundation and only affect the region close to the tunnel. Moreover, during these tests, the soil particles are assumed to receive same excitation, while in actual the propagation of vibrations appears more localized and discrete (Zhuang *et al.* 2019). Besides, analysis and explanation in these studies have been established in the view of solid mechanics, as conceptions of dynamic modulus, damping ratio, and permeability have been introduced. Yet the properties of liquefied soil after loading are more similar to the fluid, viscous fluid characteristics and rheological properties of soft soil subjected to vibrations should be taken into consideration.

Given the poor performance and inconvenience of triaxial tests for soil samples with high water content, drag tests have been performed by former researchers to investigate the flow characteristics of soft soil (Atapattu *et*

*Corresponding author, Professor
E-mail: yindeshun72@163.com

ISSN: 2005-307X (Print), 2092-6219 (Online)

al. 1990, Jossic and Magnin 2001). By assuming the soil as viscous fluids, some classic theories of fluid mechanics, such as the Stokes law and the flow theory at low Reynolds number, have been employed to estimate the viscosity of soil (Chafe and de Bruyn 2005). Hwang *et al.* (2006) found that the viscosity of the liquefied soil decreased with rising shear strain rate through a series of drag ball tests, and the non-Newtonian characteristic of soil foundations was observed to significantly affect the stability of piles. Hadush *et al.* (2000) and Sueng (2013) have derived several models to describe and predict the viscous behaviors of different sorts of soil, which fit well with their experimental data. Nevertheless, these models are either modified from classical viscous models (e.g., Bingham model) or empirical formulations of experimental data, hardly reflecting the impact of the vibrations and the properties of soft soil. Thus, a new method for predicting the flow characteristics of soft soil based on the laboratory tests is required, which is ought to take full consideration of the traits of the vibration.

Recently, one of the machine-learning methods, artificial neural network (ANN), has generated considerable research interests as a promising tool to capture the non-linear mapping relations among high-dimensional variables, with the advantages of memory simulation and high accuracy (Aminian 2017, Moayedi *et al.* 2020). In contrast with traditional linear and non-linear regression methods, no pre-defined model concepts are required in ANN, and its unique pattern which resembles the biological nervous systems has decreased the limitations on the number of inputs and outputs (Ansari *et al.* 2018). In past decades, ANN has been deemed as a strong approach to capture the complicated properties of soil, rocks, and other materials (Achieng 2019, Arel 2012, Nazari *et al.* 2015, Omari *et al.* 2020). For instance, Zhang *et al.* (2020) accurately predicted the thermal conductivity of unsaturated soil using a screened ANN method, and various influence factors such as soil fabric, water content, dry density, and soil mineralogy were considered in the process. Fernandes *et al.* (2020) established an ANN model to estimate the soil penetration resistance which is significantly affected by soil moisture, and the simulated results were further used to evaluate the soil compaction. In view of these successful attempts on modeling multi-input and non-linear problems via ANN models, it is reasonable to consider the adoption of ANN techniques on the description of flow characteristics of soft soil subjected to vibrations, and quantitatively capture the influence of multiple experimental variables.

In this paper, we conducted a series of drag-sphere tests to investigate the flow ability of soft soil subjected to vibrations with different frequencies. On the basis of obtained experimental data, an artificial neural network (ANN) model was established to predict the soil viscosity. Then, the optimal topology, training algorithm, and transfer functions were determined by comparing the simulated results with the experimental data to achieve the best prediction. Ultimately, the influence of each input on output was discussed after the contributions of experimental variables were analyzed.

2. Laboratory drag-sphere tests

To investigate flow characteristics of soft soil subjected to vibrations inside the soil body, a modified drag-sphere test device is adopted in this work. Fig. 1 displays the schematic diagram of the drag-sphere test apparatus, which was designed to measure the viscosity of liquified soil, and the photo of the test apparatus is presented in Fig. 2. Generally, the entire drag-sphere experimental system containing five parts: vibration device, soil container, power system, data acquisition system, and pressure equipment. The soil container is a steel cylinder of 260 mm in diameter and 400 mm in height. The steel sphere (20 mm in diameter) with a smooth surface was dragged on a steel track which was set 50 mm above the bottom in the container and was connected with a stepping motor which controls the drag force and moving speed. To simulate the vibrations originated from underground tunnels embedded in soil foundations, the vibrator motor was buried inside the soil and was placed 20mm above the sphere. Besides, a rubber airbag and pressure sensors were used to control the confining pressure of the underground soil.

According to Hwang *et al.* (2006), when the smooth sphere was dragged by a stable force T inside homogenous and isotropic viscous fluids in a constant speed v, the viscous resistance on the sphere can be derived through the flow theory of a low Reynolds number uniform flow as

$$F = T = 6\pi\eta vr \tag{1}$$

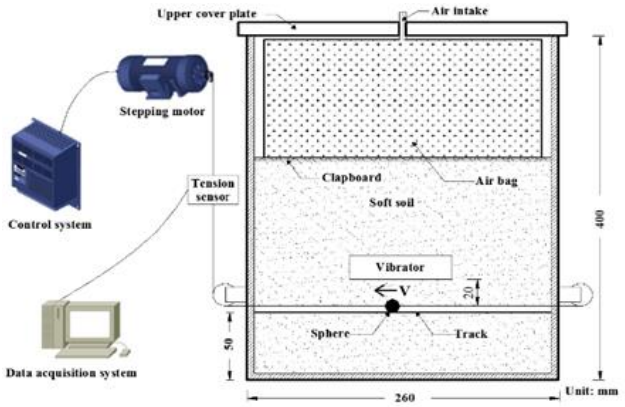

Fig. 1 Schematic diagram of experimental apparatus

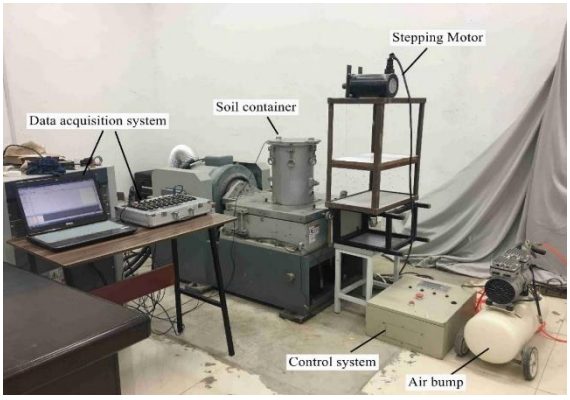

Fig. 2 Photo of drag-sphere test apparatus

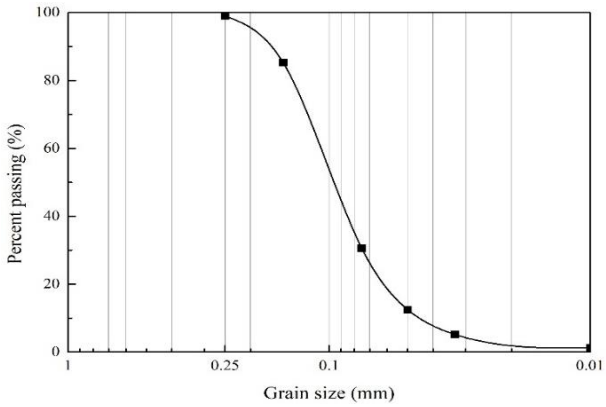

Fig. 3 Grain size distribution of testing soil samples

Table 1 Physical properties of soil samples taken from Qinghuai River region

Unit weight $\gamma(kN/m^3)$	Water content w (%)	Void ratio e	Plastic limit w_p (%)	Liquid limit w_l (%)
15.05	52.37	1.25	16.72	29.46

Table 2 Summary of experiments conducted

Independent parameters	Water content (%)	Frequency (Hz)	Confining pressure (kPa)
	42, 47, 52	0, 5, 15, 25, 35	0, 8, 20, 30

in which F is the viscous resistance, r is the radius of the smooth sphere, η is the viscosity of fluid-like soil. Refer to the principles proposed by Chhabra and Richardson (2008), the viscous resistance equals to the skin friction of sphere when the moving velocity is relatively low. Therefore in our study the dragging speed was set to be $v_0 = 48\ mm/min$, and the viscosity can be expressed as

$$\eta = \frac{T}{6\pi vr} \tag{2}$$

The soil samples were collected from a foundation pit of a constructing metro project near Qinhuai River, in the city of Nanjing, China. Fig. 3 displays the grain size distribution of soil samples, and main physical properties of the test samples are listed in Table 1. In order to investigate the influence of the moisture content, the soil samples were dried and reconstituted with three levels of water content: 42%, 47%, and 52%. Besides, the confining pressure was set to four levels: 0 kPa, 8 kPa, 20 kPa, and 30 kPa, to mimic the soil body in different depth. As reported by Tang *et al.* (2008), the vibration frequency of an operating underground train varies from 15 Hz to 50 Hz which depends on its velocity, so five vibration frequencies (5 Hz, 15 Hz, 25 Hz, 35 Hz, and 45 Hz) were adopted in this work. Table 2 presents the summary of experimental conditions and treatments for the soil samples

The viscosity curves of all tested soil samples are shown in Fig. 4. Apparently, the viscosity decreases under vibrations of higher frequencies for all samples, which indicates that the soil sample was transformed into a fluid-like state due to the mechanical vibrations. According to Yang *et al.* (2014), the reduction of viscosity may be

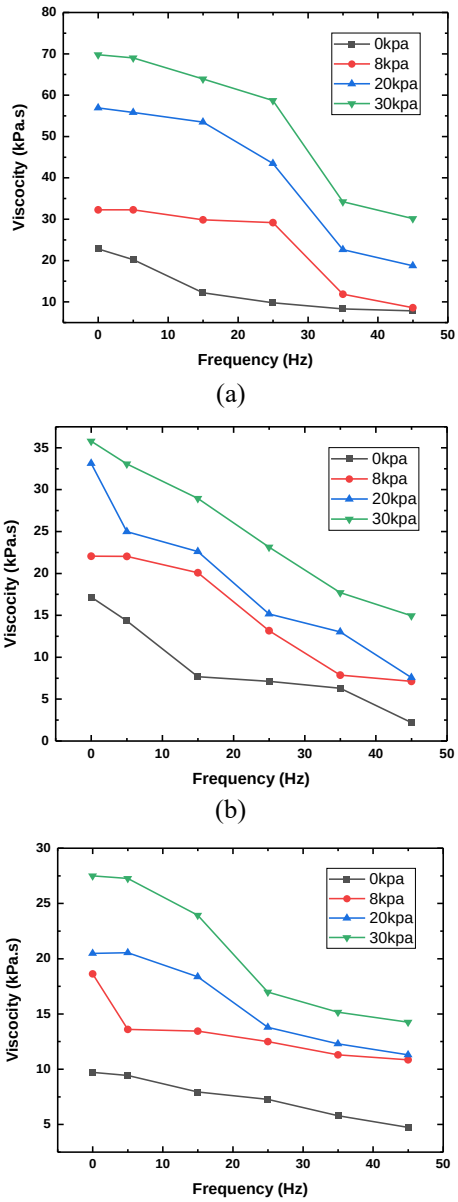

Fig. 4 Viscosity curves of soft soil samples subjected to vibrations of different frequencies under different confining pressure. The moisture content of testing soil samples is: (a) 42%, (b) 47% and (c) 52%

induced by the mechanical vibration which motivates the water molecules and soil aggregates to vibrate and collide with each other, and such collision could have separated the aggregates or even broke the structure of soil when the frequency is relatively high. Besides, it is also noteworthy that under higher confining pressure, the viscosity of soil samples is comparatively high, demonstrating that the confining pressure has weakened the flow ability of the soil samples.

3. Artificial neural network model

Artificial neural network (ANN) simulates the

Table 3 Training algorithms and transfer functions applied in the network

Training Algorithm	Transfer Function
Levenberg-Marquardt (LM)	Tan-sigmoid (Tansig)
Scaled Conjugate Gradient (SCG)	Log-sigmoid (Logsig)
Bayesian Regulation back propagation (BR)	Hard-limit (Hardlim)
Resilient back Propagation (RP)	Pure-linear (Purelin)

Table 4 Values of parameters in the GA algorithm

Algorithm	Population size	Number of iterations	Crossover probability	Mutation probability
GA	10	100	0.4	0.2

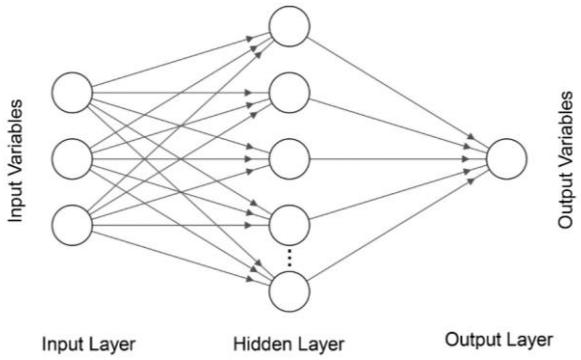

Fig. 5 Architecture of artificial neural network with one hidden layer

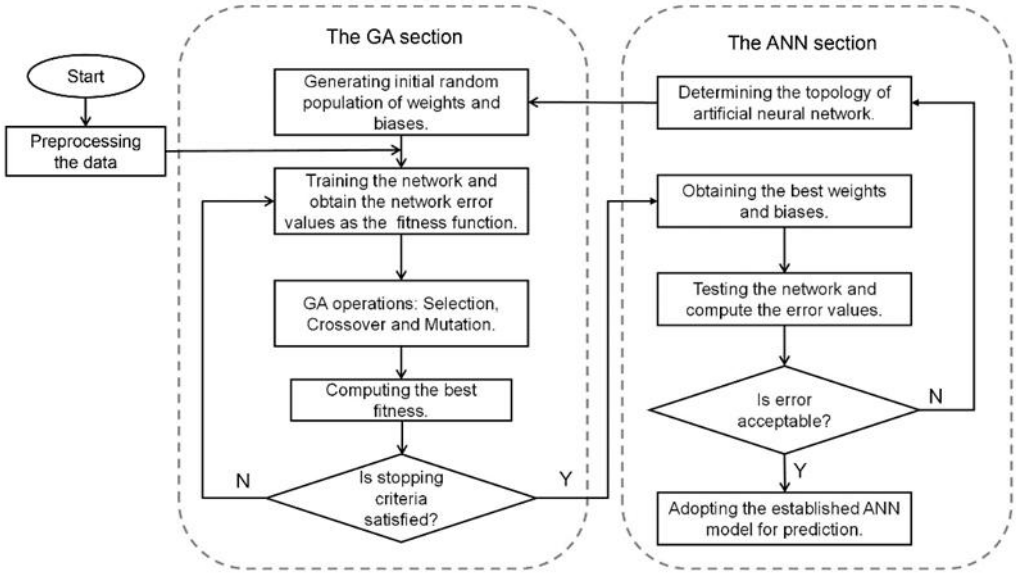

Fig. 6 Flow chart of the overall GA-ANN algorithm

biological nervous systems, consisting of a number of units/neurons and the weighted connections between them (Hemmat Esfe *et al.* 2017). As shown in Fig. 5, generally these units/neurons are arranged in three sorts of layers. The input layer receives all the input variables, and the output layer provides the network's outputs, while the rest of the neurons form the hidden layer, which transforms the weight values receiving from the input layer through a transfer function and then passes the results to the output layer. In most ANN models, structures are not fixed and rely on the specific problem to be solved. Normally for an artificial neural network, the process of computing outputs for each neuron in the hidden layer can be expressed as

$$y_j = f\left(\sum_{j=1}^{n} w_{ji}x_i + b_j\right) \tag{3}$$

where y_j means the output from the *j*th neuron/unit, *f* is the transfer function, x_i is the *i*th input vector to the *j*th neuron/unit, w_{ji} denotes the weight factor between the *i*th neuron/unit and the *j*th neuron/unit, b_j is the bias of the *j*th neuron/unit, *n* is the number of all neuron/units in hidden layer.

In general, the main procedure of establishing an ANN model can be divided into three parts: (1) determining the architecture of the network; (2) finding suitable transfer functions and training algorithms; (3) selecting the optimal weights and biases. In this work, the model has three independent inputs (water content, frequency, and confining pressure) and one output (viscosity), which denotes that there are three neurons in the input layer and one neuron in the output layer. As reported by Cybenko (1989), arbitrary continuous functions can be approximated by feedforward neural networks with only one hidden layer and sigmoidal transfer function, and the use of two or more hidden layers exacerbates the problem of local minima, thus one hidden layer is adequate for our network considering the inputs and output are not complicated. Generally, too less neurons in hidden layer result in higher training and generalization errors, while excessive neurons will overestimate the complexity of the target problem and lead to over-fitting in prediction or interpolation (Sheela *et al.* 2013). Up to now, even efforts have been made on fixing the number of hidden neurons (Yuan *et al.* 2003, Sartori and Antsaklis 1991, Zhang *et al.* 2004), the scientific communities have not yet reached an agreement regarding the most appropriate method to determine the optimal hidden neurons, as the network architecture, the degree of noise, and the complexity of the function have to be taken into account. With regard to this work, statistical analysis on the performance of networks with different number of hidden neurons are conducted and the result with the minimum estimated generalization error is determined as the optimum. Besides, various prevalent training algorithms and transfer functions are applied in this study, which are listed in Table 3, and the suitable form of training algorithm and transfer function will be determined by comparing the simulation results with the experimental data.

Genetic algorithm (GA) is one of the most effective global search techniques which is inspired by the Darwin's biological evolution principle and has been applied in solving many optimization problems (Rahimi *et al.* 2015, Zaji *et al.* 2020). As random selections of weights and biases may result in local minima and slow convergence of the ANN model, it is practicable to optimize the weights and biases through GA to reach closer to the target values. Commonly, the GA optimization starts with a primary set of values (population) and evolves through iterations including selection, crossover, and mutation operations. More detailed information on the steps involved in GA optimization can be found in Beigzadeh *et al.* (2013) 's article. Refer to some previous studies (Rahimi *et al.* 2015, Karimi and Yousefi 2012, Beigzadeh *et al.* 2013) and regarding our experimental data, the values of the key parameters (population size, number of iterations, crossover probability, and mutation probability) are defined and listed in Table 4. And the flow chart of the overall GA-ANN training algorithm is presented in Fig. 6

4. Results and discussion

A three-layer GA-ANN model has been employed to describe the nonlinear relation between viscosity and three influence factors: water content, frequency, and confining pressure. Specifically, as 72 data points were obtained from the drag-sphere tests, 51 data points are employed to train the model, and the rest 21 data points are adopted to test the model to ensure the reliability. In this study, the MATLAB software produced by MathWorks is used to develop the proposed model. In order to improve the model accuracy, all inputs and outputs were pre-processed and scaled between [-1,1] by means of a built-in MALAB function (mapminmax) before running the model. And after finishing the training and predicting process, the predicted viscosities are recovered to their original values through the reverse-normalization using the same function. In addition, to assess the performance of ANN model, the mean square error (MSE) is exerted to determine the model accuracy and the coefficient of determination (R^2) is adopted to depict the correlation between model prediction and experimental data, which are defined as

$$R^2 = \frac{\sum_{i=1}^{N}\left(y_i^{exp} - \bar{y}\right)^2 - \sum_{i=1}^{N}\left(y_i^{exp} - y_i^{pre}\right)^2}{\sum_{i=1}^{N}\left(y_i^{exp} - \bar{y}\right)^2} \tag{4}$$

$$MSE = \frac{1}{N}\sum_{i=1}^{N}\left(y_i^{exp} - y_i^{pre}\right)^2 \tag{5}$$

where y_i^{exp} is the *i*th value of experimental viscosity, y_i^{pre} is the *i*th predicted value of viscosity by ANN model, $\bar{y}$ is the average value of experimental viscosity, and *N* denotes the number of experimental data points.

Table 5 displays the performance of the GA-ANN model with four different training algorithms, where the number of neurons in the hidden layer was set to be 5. Obviously, the model adopting Levenberg-Marquardt (LM) algorithm gives more accurate descriptions of the training data than the other three, as the value of MSE is closer to 0 and the value of R2 approaches to 1, while its performance on processing the testing data is not so satisfactory. Among the other three, the more superior values of MSE and R^2 for both training and testing data sets of models with Resilient back Propagation (RP) algorithm indicate that the RP algorithm is a proper choice for the present model. Thus, the RP algorithm is selected to conduct the research subsequently.

Learning rate is a significant parameter of the GA-ANN model, as it is widely recognized that the performance of the neural network is very sensitive to the value of the learning rate. If the learning rate is too small, the algorithm will take a very long time to converge. On the other hand, if very large learning rate is taken, the algorithm may oscillate and result in unstable learning since it may step over a minimum (Fang *et al.* 2005). Fig. 7 presents the comparison of the convergence time and model performance of three-layer ANN models adopting different learning rate: 0.05,

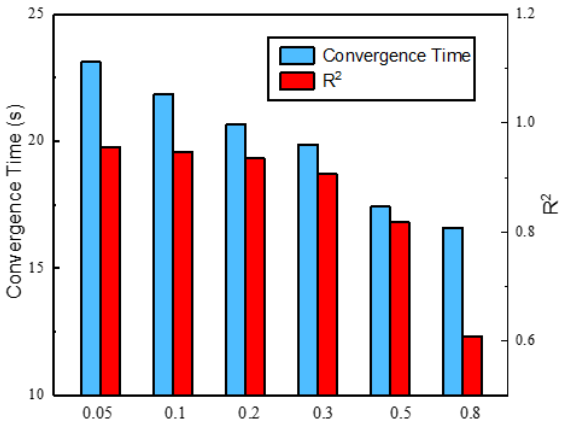

Fig. 7 Comparison of the convergence time and model

Table 5 Performance of the GA-ANN model with different training algorithms

Algorithm	Training data sets		Testing data sets	
	MSE	R^2	MSE	R^2
LM	0.000432	0.9977	0.0369	0.8938
SCG	0.0021	0.9869	0.0228	0.9401
BR	0.0032	0.9849	0.0193	0.9293
RP	0.002	0.987	0.0173	0.9549

Table 6 Performance of the ANN model with different transfer functions

Group index	Transfer function	Training data sets		Testing data sets	
		MSE	R^2	MSE	R^2
1	Tansig+Logsig	0.3761	0.1941	0.3116	0.3555
2	Tansig+Tansig	0.001	0.995	0.056	0.8549
3	Tansig+Hardlim	0.3457	0.2608	0.3717	0.3744
4	Tansig+Purelin	0.000432	0.9977	0.0369	0.8938
5	Logsig+Logsig	0.2964	0.3336	0.5509	0
6	Logsig+Tansig	0.000782	0.9963	0.1541	0.6473
7	Logsig+Hardlim	0.3994	0	0.423	0
8	Logsig+Purelin	0.0014	0.9943	0.0434	0.8439

0.1, 0.2, 0.3, 0.5 and 0.8. Evidently, as the learning rate increases, the model converges quickly while the accuracy of the predictions on testing dataset continues to decline.

Considering both the acceptable running cost and the decent model performance, the learning rate of 0.1 is adopted in this research.

performance of ANN models with different learning rate: 0.05, 0.1, 0.2, 0.3, 0.5 and 0.8.

Table.6 presents the performance of the proposed model with different combinations of transfer functions. As reported by Maier and Dandy (2000), adopting sigmoidal-type functions in the hidden layers can improve extrapolation ability of ANN to a great extent. Previous studies (Achieng 2019, Mojid *el al.* 2019, Zhang *et al.* 2020 indicate that Tan-sigmoid (Tansig) and Log-sigmoid (Logsig) functions have been prevalent selections as the transfer function between the input layer and the hidden layer, and in this study we also considered the other two frequently-used functions (Pure-linear and Hard-limit) as the transfer function between the hidden layer and the output layer, (here we don't list the case of using these two functions in the input-hidden layer due to the large prediction error and meaningless computing cost), which brings total 8 combinations of transfer functions into calculation. The simulation results show that the fourth group of transfer functions, which consists of Tan-sigmoid and Pure-linear functions, provides the minimum error and the best correlations both for the training dataset and testing dataset. Accordingly, it is reasonable to adopt such transfer functions in the network to achieve high accuracy.

Fig. 8 shows the performance of GA-ANN models with different number of neurons in the hidden layer, where the relations of neuron numbers and the value of MSE and R2 for both training and testing datasets are presented. Concretely, as the hidden layer comprises more neurons, the ability of the model to fit the training data gets stronger straightly. However, as seen from Fig.8 (b), merely increasing neurons results in overfitting, a phenomenon that the training samples are well-simulated but it fails to depict the testing data accurately, as the value of MSE rises and the value of R^2 drops when more than 10 neurons were employed in the hidden layer for the testing dataset. Taken together, the model structure with 6 neurons in the hidden layer is acceptable in view of its relatively excellent in fitting both the training and testing datasets.

After the topology, transfer functions, and training algorithm have been determined, the proposed model is trained and used for prediction. Fig. 9 demonstrates the results obtained from the GA-ANN model against the experimental data. The value of MSE for training data and testing data is 0.0023 and 0.0185 respectively, denoting that our model is quite accurate with a tiny fitting error. And the value of R^2, which is 0.9868 for the training data and 0.9471 for the testing data, also shows that there is a proper agreement between the prediction and experimental results. Furthermore, we compared the performance of the proposed GA-ANN model with a classical ANN model to examine the improvement of using genetic algorithm. The adopted basic three-layer ANN model was directly established by using the ready package in Machine Learning toolbox of MATLAB, with six neurons in the hidden layer. As listed in Table.7, the GA-ANN model converges faster and shows better predictive validity than the basic ANN model, which proves that the deployment of genetic algorithm has obviously improved the predictive ability of ANN models. Thus, the proposed GA-ANN model can be used to depict the nonlinear relations between viscosity and three influence factors (water content, frequency, and confining pressure) and predict the possible value of viscosity without further experiments.

Table 7 Comparison of the performance of ANN and GA-ANN models

Model	Convergence Time (s)	MSE	R^2
ANN	26.31	0.197	0.6225
GA-ANN	21.87	0.0185	0.9471

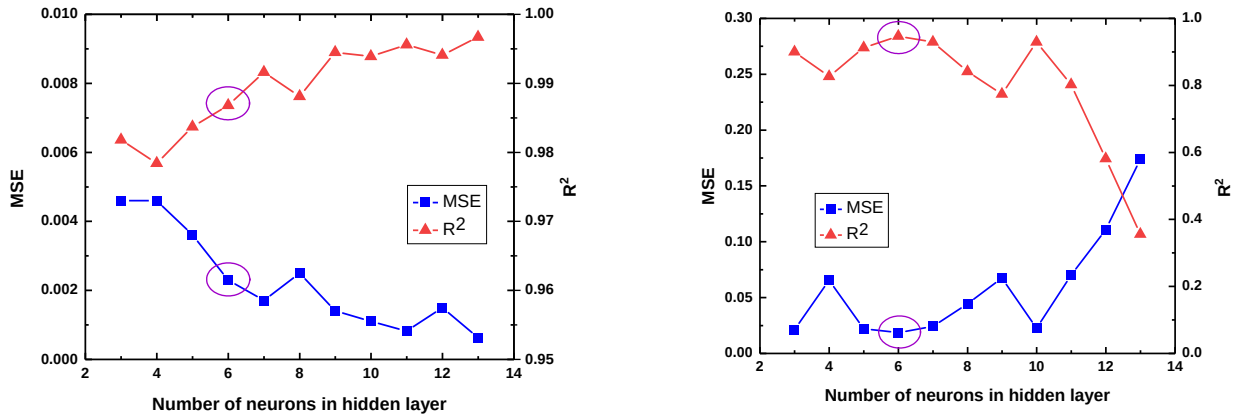

Fig. 8 Performance of GA-ANN models with different number of neurons in the hidden layer for: (a) training data sets and (b) testing data sets

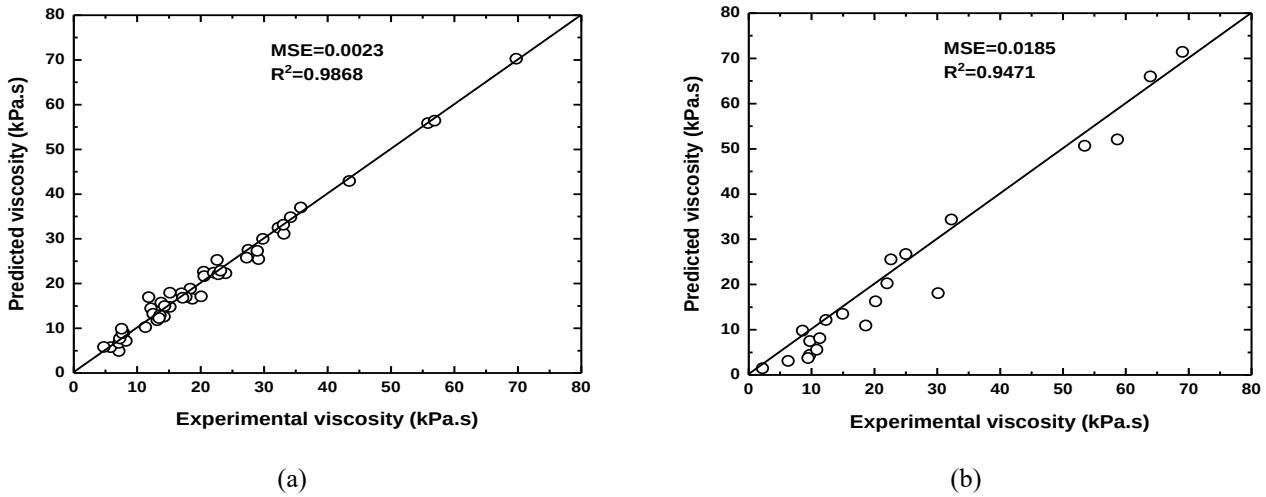

Fig. 9 Comparison of predictions by GA-ANN model and experimental viscosity for: (a) training data sets and (b) testing data sets

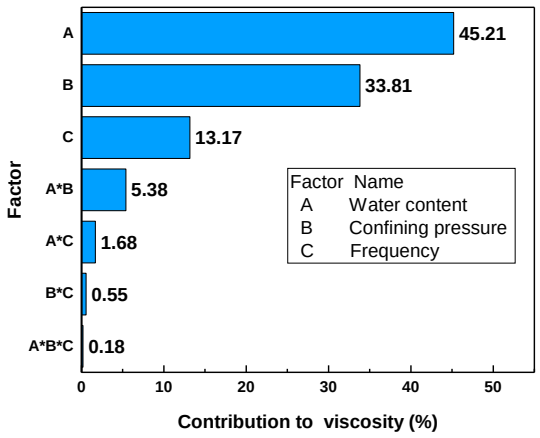

Fig. 10 Contributions of the factors on the calculated viscosity

To investigate the effect of each input on output and the interactions of input variables, multivariate analysis of variance (MANOVA) is used to analyze the contributions of the factors. As one of the traditional methods of data analysis, MANOVA tests the statistical significance of a particular main effect or an interaction on each of the response measurement, as well as the significance of the overall effect, which provides us a way of quantitative description to the whole dataset (Liu 2016). By processing the input and output data in SPSS software, contributions of

the factors and their interactions on the calculated viscosity are obtained. As shown in Fig.10, the water content accounts for the dominant factor that dominantly influences the viscosity while the frequency of the vibration has the minimum effect for a single factor on the viscosity. This corresponds to the fact that altering the water content of soft soil directly affects its flow ability. Besides, the interaction between the water content and confining pressure also affects the viscosity while the rest of the interactions have little impact. These findings reveal that it is the natural properties and geological conditions that influence the flow characteristics of soft soil more than the applied vibrations.

Furthermore, the analytical results of contributions of each input also provide new perspectives for designing and conducting laboratory experiments. For instance, as the water content is proved to be the dominant factor, it is reasonable to prepare more soil samples with a large range of water content (e.g., 5% to 95%), which is able to obtain more precise and complete testing results of the flow characteristic of the soil samples.

5. Conclusions

In this research, an experimental investigation based on drag-sphere tests and artificial neural network modelling techniques were carried out to evaluate the flow characteristics of soft soil subjected to vibrations. The drag-sphere tests for soft soil samples under different water content, vibration frequency, and confining pressure were conducted, and the results show that the flow ability of soil samples rises under lower confining pressure and vibrations with higher frequencies. On the basis of the experimental data, an artificial neural network (ANN) was built to predict the measured viscosity, where a genetic algorithm (GA) was adopted to improve the model performance by optimizing the values of weights and biases. Preliminary trials on ANN models with different learning rate demonstrate that the model converges fast and exhibits excellent prediction ability when the learning rate was set to 0.1. By comparing the predicted results with the experimental data, it was found that the Resilient back Propagation (RP) is the best training algorithm and the combination of Tan-sigmoid (Tansig) function and Pure-linear (Purelin) function are the proper transfer functions for the network. Further analysis on the performance of GA-ANN models with different number of neurons in the hidden layer reveals that the three-layer network with 6 neurons in the hidden layer is the optimal structure for the established model, as blindly increasing neurons results in undesirable overfitting. The predictions show that there is a terrific agreement between the established GA-ANN prediction and the experimental data. Besides, the effect of the three inputs on outputs was also investigated by means of multivariate analysis of variance, and it was demonstrated that the main factor affecting viscosity is the water content and the frequency has the minimum impact for a single factor, while the interactions of the three inputs are almost negligible, except for the interactions between the water content and the confining pressure. This finding corresponds to the fact that the flow ability of soft soil is mainly affected by the geological conditions and its natural properties, which may provide guidance on the designing laboratory tests.

Acknowledgments

The authors acknowledge the funding support from the National Natural Science Foundation of China (Grant No. 11872173) and Shenzhen Science and Technology Plan Project (JSGG20180507183020876).

References

Achieng, K.O. (2019), "Modelling of soil moisture retention curve using machine learning techniques: Artificial and deep neural networks vs support vector regression models", *Comput. Geosci.*, **133**, 104320, https://doi.org/10.1016/j.cageo.2019.104320.

Al-Bared, M.A.M., Harahap, I.S.H., Marto, A., Abad, S.V.A.N. and Ali, M.O.A. (2019), "Undrained shear strength and microstructural characterization of treated soft soil with recycled materials", *Geomech. Eng.*, **18**(4), 427-437. https://doi.org/10.12989/gae.2019.18.4.427.

Aminian, A. (2017), "Predicting the effective viscosity of nanofluids for the augmentation of heat transfer in the process industries", *J. Mol. Liq.*, **229**, 300-308. https://doi.org/10.1016/j.molliq.2016.12.071.

Ansari, H.R., Zarei, M.J., Sabbaghi, S. and Keshavarz, P. (2018), "A new comprehensive model for relative viscosity of various nanofluids using feed-forward back-propagation MLP neural networks", *Int. Commun. Heat Mass.*, **91** 158-164. https://doi.org/10.1016/j.icheatmasstransfer.2017.12.012.

Arel, E. (2012), "Predicting the spatial distribution of soil profile in Adapazari/Turkey by artificial neural networks using CPT data", *Comput. Geosci.*, **43**, 90-100. https://doi.org/10.1016/j.cageo.2012.01.021.

Atapattu, D D., Chhabra, R.P. and Uhlherr, P.H.T. (1990), "Wall effect for spheres falling at small reynolds number in a viscoplastic medium", *J. Non-Newton Fluid*, **38**(1), 31-42. https://doi.org/10.1016/0377-0257(90)85031-S.

Beigzadeh, R., Rahimi, M. and Parvizi, M. (2013), "Experimental study and genetic algorithm-based multi-objective optimization of thermal and flow characteristics in helically coiled tubes", *Heat Mass Transfer*, **49**(9), 1307-1318. https://doi.org/10.1007/s00231-013-1176-1.

Chafe, N.P. and de Bruyn, J.R. (2005), "Drag and relaxation in a bentonite clay suspension", *J. Non-Newton Fluid*, **131**(1), 44-52. https://doi.org/10.1016/j.jnnfm.2005.08.010.

Chen, G., Wang, Z., Zuo, X., Du, X. and Gao, H. (2013), "Shaking table test on the seismic failure characteristics of a subway station structure on liquefiable ground", *Earthq. Eng. Struct. D*, **42**(10), 1489-1507. https://doi.org/10.1002/eqe.2283.

Chhabra, R.P. and Richardson, J.F. (2008), *Chapter 1*, *Non-Newtonian Fluid Behaviour*, 1-55.

Cybenko, G. (1989), "Approximation by superpositions of a sigmoidal function", *Math. Control Signal. Syst.*, **2**(4), 303-314. https://doi.org/10.1007/BF02551274.

Fang, X., Luo, H., Tang, J., (2005). "Structural damage detection using neural network with learning rate improvement". *Comput. Struct.*, **83**(25-26), 2150-2161. https://doi.org/10.1016/j.compstruc.2005.02.029.

Fernandes, M.M.H., Coelho, A.P., Silva, M.F.D., Bertonha, R.S., Queiroz, R.F.D., Furlani, C.E.A. and Fernandes, C. (2020), "Estimation of soil penetration resistance with standardized moisture using modeling by artificial neural networks", *Catena*,

189, 104505, https://doi.org/10.1016/j.catena.2020.104505.

Hemmat Esfe, M., Bahiraei, M., Hajmohammad, M.H. and Afrand, M. (2017), "Rheological characteristics of MgO/oil nanolubricants: Experimental study and neural network modeling", *Int. Commun. Heat Mass Transfer*, **86** 245-252, https://doi.org/10.1016/j.icheatmasstransfer.2017.05.017.

Huang, J., Yuan, T., Peng, L., Yu, J. and Ding, Z. (2015), "Model test on dynamic characteristics of invert and foundation soils of high-speed railway tunnel", *Earthq. Eng. Eng. Vib.*, **14**(3), 549-559. https://doi.org/10.1007/s11803-015-0044-z.

Huang, Z., Pitilakis, K., Tsinidis, G., Argyroudis, S. and Zhang, D. (2020), "Seismic vulnerability of circular tunnels in soft soil deposits: The case of Shanghai metropolitan system", *Tunn. Undergr. Sp. Tech.*, **98**, 103341. https://doi.org/10.1016/j.tust.2020.103341.

Hwang, J., Kim, C., Chung, C. and Kim, M. (2006), "Viscous fluid characteristics of liquefied soils and behavior of piles subjected to flow of liquefied soils", *Soil Dyn. Earthq. Eng.*, **26**(2), 313-323. https://doi.org/10.1016/j.soildyn.2005.02.020.

Jeong, S.W. (2013), "Determining the viscosity and yield surface of marine sediments using modified Bingham models", *Geosci. J.*, **17**(3), 241-247. https://doi.org/10.1007/s12303-013-0038-7.

Jossic, L. and Magnin, A. (2001), "Drag and stability of objects in a yield stress fluid", *AICHE J.*, **47**(12), 2666-2672. https://doi.org/10.1002/aic.690471206.

Karimi, H. and Yousefi, F. (2012). "Application of artificial neural network-genetic algorithm (ANN-GA) to correlation of density in nanofluids". *Fluid Phase Equilibr.*, **336**, 79-83. https://doi.org/10.1016/j.fluid.2012.08.019.

Kheirbek-Saoud, S. and Fleureau, J. (2012), "Liquefaction and post-liquefaction behaviour of a soft natural clayey soil", *Geomech. Eng.*, **4**(2), 121-134, 10.12989/gae.2012.4.2.121.

Kumar, S.S., Krishna, A.M. and Dey, A. (2018), "Dynamic properties and liquefaction behaviour of cohesive soil in northeast India under staged cyclic loading", *J. Rock Mech. Geotech. Eng.*, **10**(5), 958-967. https://doi.org/10.1016/j.jrmge.2018.04.004.

Liu, J., Wang, T. and Tian, Y. (2010), "Experimental study of the dynamic properties of cement- and lime-modified clay soils subjected to freeze-thaw cycles", *Cold Reg. Sci. Technol.*, **61**(1), 29-33. https://doi.org/10.1016/j.coldregions.2010.01.002.

Liu, X. (2016), *Methods and Applications of Longitudinal Data Analysis*, Academic Press, Oxford, England, U.K.

Maier, H.R. and Dandy, G.C. (2000), "Neural networks for the prediction and forecasting of water resources variables: A review of modelling issues and applications", *Environ. Modell. Softw.*, **15**(1), 101-124. https://doi.org/10.1016/S1364-8152(99)00007-9.

Moayedi, H., Gör, M., Lyu, Z. and Bui, D.T. (2020), "Herding Behaviors of grasshopper and Harris hawk for hybridizing the neural network in predicting the soil compression coefficient", *Measurement*, **152** 107389. https://doi.org/10.1016/j.measurement.2019.107389.

Mojid, M.A., Hossain, A.B.M.Z. and Ashraf, M.A. (2019), "Artificial neural network model to predict transport parameters of reactive solutes from basic soil properties", *Environ. Pollut.*, **255**(2). https://doi.org/10.1016/j.envpol.2019.113355.

Moss, R.E.S. and Crosariol, V.A. (2013), "Scale model shake table testing of an underground tunnel cross section in soft clay", *Earthq. Spectra*, **29**(4), 1413-1440. https://doi.org/10.1193/070611EQS162M.

Nazari, A., Rajeev, P. and Sanjayan, J.G. (2015), "Offshore pipeline performance evaluation by different artificial neural networks approaches", *Measurement*, **76** 117-128. https://doi.org/10.1016/j.measurement.2015.08.035.

Omari, M.A., Almagableh, A., Sevostianov, I., Ashhab, M.S. and Yaseen, A.B. (2020), "Modeling of the viscoelastic properties of thermoset vinyl ester nanocomposite using artificial neural network", *Int. J. Eng. Sci.*, **150**, 103242. https://doi.org/10.1016/j.ijengsci.2020.103242.

Rahimi, M., Hajialyani, M., Beigzadeh, R. and Alsairafi, A.A. (2015), "Application of artificial neural network and genetic algorithm approaches for prediction of flow characteristic in serpentine microchannels", *Chem. Eng. Res. Des.*, **98**, 147-156. https://doi.org/10.1016/j.cherd.2015.05.005.

Sartori, M.A. and Antsaklis, P.J. (1991), "A simple method to derive bounds on the size and to train multilayer neural networks", *IEEE T. Neural Networ.*, **2** (4), 467-471. https://doi.org/10.1109/72.88168.

Sheela, K.G. and Deepa, S.N. (2013), "Review on methods to fix number of hidden neurons in neural networks", *Math. Probl. Eng.* https://doi.org/10.1155/2013/425740.

Shih, J.Y., Thompson, D.J. and Zervos, A. (2017), "The influence of soil nonlinear properties on the track/ground vibration induced by trains running on soft ground", *Transport. Geotech.*, **11**, 1-16. https://doi.org/10.1016/j.trgeo.2017.03.001.

Tang, Y., Cui, Z., Zhang, X. and Zhao, S. (2008), "Dynamic response and pore pressure model of the saturated soft clay around the tunnel under vibration loading of Shanghai subway", *Eng. Geol.*, **98**(3), 126-132. https://doi.org/10.1016/j.enggeo.2008.01.014.

Xu, Q., Ou, X., Au, F.T.K., Lou, P. and Xiao, Z. (2016), "Effects of track irregularities on environmental vibration caused by underground railway", *Eur. J. Mech. A Solid*, **59**, 280-293. https://doi.org/10.1016/j.euromechsol.2016.04.005.

Yang, W., Tan, S.K., Wang, H. and Yu, G. (2014), "Rheological properties of bed sediments subjected to shear and vibration loads", *J. Waterw. Port Coast*, **140**(1), 109-113. https://doi.org/10.1061/(ASCE)WW.1943-5460.0000211.

Yang, Y.B. and Hung, H.H. (2008), "Soil vibrations caused by underground moving trains", *J. Geotech. Geoenviron.*, **134**(11), 1633-1644. https://doi.org/10.1061/(ASCE)1090-0241(2008)134:11(1633).

Yuan, H.C., Xiong, F.L. and Huai, X.Y. (2003), "A method for estimating the number of hidden neurons in feed-forward neural networks based on information entropy", *Comput. Electron. Agr.*, **40**(1-3), 57-64. https://doi.org/ 10.1016/S0168-1699(03)00011-5.

Zaji, A.H., Bonakdari, H., Khameneh, H.Z. and Khodashenas, S. R. (2020), "Application of optimized artificial and radial basis neural networks by using modified genetic algorithm on discharge coefficient prediction of modified labyrinth side weir with two and four cycles", *Measurement*, **152**, 107291. https://doi.org/10.1016/j.measurement.2019.107291.

Zhang, N., Zou, H., Zhang, L., Puppala, A.J., Liu, S. and Cai, G. (2020), "A unified soil thermal conductivity model based on artificial neural network", *Int. J. Therm. Sci.*, **155**, 106414. https://doi.org/10.1016/j.ijthermalsci.2020.106414.

Zhang, Z.Z., Ma, X.M. and Yang, Y.X., (2004), "Bounds on the number of hidden neurons in three-layer binary neural networks (vol 16, pg 995, 2003)", *Neural Networks*, **17**(3), 465-465. https://doi.org/10.1016/j.neunet.2004.01.001.

Zhongxun, Z., Deshun, Y., Chunyu, B. and Chao, Z. (2019), "Influence of sand content on the flow characteristics of soft soil under cyclic and high-frequency vibration", *Earthq. Eng. Eng. Vib.*, **18**(3), 487-496. https://doi.org/10.1007/s11803-019-0516-7.

Zhu, Q., Jin, Y., Shang, X. and Chen, T. (2019), "A 1D model considering the combined effect of strain-rate and temperature for soft soil", *Geomech. Eng.*, **18**(2), 133-140. https://doi.org/10.12989/gae.2019.18.2.133.

CC